Electron-hole counts in Al-substituted MgB_2 superconductors from x-ray Raman scattering

A. Mattila,[1,2,*] J. A. Soininen,[1] S. Galambosi,[1] T. Pylkkänen,[3] S. Huotari,[3] N. D. Zhigadlo,[4] J. Karpinski,[4] and K. Hämäläinen[1]

[1]*Department of Physics, University of Helsinki, P.O. Box 64, 00014 Helsinki, Finland*

[2]*STUK – Radiation and Nuclear Safety Authority, P.O. Box 14, 00881 Helsinki, Finland*

[3]*European Synchrotron Radiation Facility, BP 220, F-38043 Grenoble Cedex, France*

[4]*Solid State Physics Laboratory, ETH, CH-8093 Zürich, Switzerland*

(Received 13 April 2007; revised manuscript received 14 May 2008; published 21 August 2008)

We have investigated the electronic structure of $Mg_{0.83}Al_{0.17}B_2$ and MgB_2 single crystals using x-ray Raman scattering at the B-K edge. Utilizing the momentum transfer dependence of the scattering process, together with first-principles multiple scattering calculations, we have extracted the site and symmetry projected density of empty B states in $Mg_{0.83}Al_{0.17}B_2$ in the presence of a core hole. In comparison to the density of states for pure MgB_2, we find the B-σ-band hole count to decrease at the Fermi level by $35\pm9\%$. The π-band hole count is relatively stable with a $4\pm7\%$ increase compared to MgB_2. These results shed light on the role of band filling in lowering the T_c. Our work opens an application area for x-ray Raman scattering and density of states extraction scheme in studies of doped systems.

DOI: 10.1103/PhysRevB.78.064517 PACS number(s): 74.25.Jb, 71.15.−m, 74.70.Ad, 78.70.Ck

I. INTRODUCTION

Atomic substitutions and doping are used to modify and engineer the physical properties of compounds and have been naturally applied to alter the superconducting properties of various systems. For understanding and predicting the effects of substitution or doping, knowledge of the electronic structure is crucial, and especially for elucidating changes in the superconductivity, the density of states at the Fermi level is an important characteristic of the system. Atomic substitutions have been also employed for MgB_2, whose high critical temperature of superconductivity $T_c \simeq 39$ K has been explained to arise from a phonon-mediated mechanism with different coupling strengths to the electronic B-σ and π bands.[1–4] Even though the different coupling strengths lead to a realization of two-band superconductivity,[5] MgB_2 still has only one transition temperature due to weak interband phonon scattering between σ and π bands.[4] The high density of empty electronic states at the Fermi level, provided by the B-σ band, is one of the essential features behind the high T_c in MgB_2. The quasi-two-dimensional (2D) σ band, deriving from the hybridized B sp_xp_y orbitals, resides within the B sheets and couples strongly to B-B E_{2g} bond oscillations,[6,7] leading to the larger superconducting energy gap. The smaller gap originates from the three-dimensional (3D) π band, formed by B p_z orbitals, with a weaker electron-phonon coupling strength.

In MgB_2, atomic substitutions can be used to change the phonon scattering rates and to modify the electronic density of states. Two studied substitutions have been the ones of Al for Mg and of C for B. Although both modifications dope the system with additional electrons, the effects on the scattering of electrons from phonons are different.[8–11] The Al substitution is expected to mostly affect the scattering in the π band, whereas C substitution should increase both the σ and π band scattering. In both cases the modification leads to a decrease in the critical temperature and the eventual disappearance of superconductivity.[12] Recent work has suggested that the lowering of the critical temperature in MgB_2 would result from the reduction of the electron phonon coupling constant due to band filling, with the π gap region staying constant due to the compensating effect of a changing interband scattering rate.[13,14] To elucidate the role of the band filling versus the changes in the phonon spectra or in the interband scattering rate, further experimental work on the substituted MgB_2 compounds is needed.

The exact details of the electron doping induced changes in MgB_2 are still uncertain, and until recently, the effect of substitution was mainly investigated on polycrystalline samples.[15–18] Single crystal MgB_2 and AlB_2 have been already characterized,[19] however high quality Al and C, substituted crystals with intermediate substitution levels, have only lately become available, enabling more detailed studies of the anisotropies.[10,11,20] In a recent de Haas–van Alphen study of Al substituted single crystal MgB_2,[14] the authors found a 16% reduction in the number of σ band holes with 7.5% Al content, but were unable to derive a number for the π band.

In this context, x-ray Raman scattering (XRS) (Ref. 21) is well suited to probe both the σ and π band hole counts on equal footing in Al substituted MgB_2 single crystals. The anisotropies and symmetries of the empty electronic states in pure MgB_2 have been already investigated using XRS[22] to separate the s, σ, and π band contributions. Later theoretical developments[23] have also made it possible to quantitatively extract the site and symmetry projected local density of states (ℓDOS) from the experimental XRS data, allowing a direct comparison to theoretical calculations of the electronic structure. The power of this scheme has already been demonstrated on pure MgB_2.[24] In the following we will extend this scheme to doped systems, opening completely new areas for the applications of x-ray Raman scattering.

In this paper we present an XRS investigation at the B-K edge on Al-substituted single crystal $Mg_{0.87}Al_{0.17}B_2$ and on pure MgB_2. We probe the electron doping-induced changes in the empty B electronic states, especially in the interesting σ and π bands. As we use hard x-rays, we probe the bulk of

the sample, which is a significant advantage, considering the hygroscopic nature of MgB_2 crystals.[25] Utilizing the momentum transfer dependence of the XRS, we quantitatively extract the s, σ, and π ℓDOS from the XRS data and discuss the evolution of the electronic structure due to Al substitution.

II. CALCULATION METHOD

In the nonrelativistic Born approximation, the double-differential cross section for nonresonant inelastic x-ray scattering is proportional to the dynamic structure factor. In XRS, core electrons are excited, and the relevant matrix element can be approximated as $\langle f|\exp(\vec{q}\cdot\vec{r})|i\rangle$, where $|i\rangle$ and $|f\rangle$ are the initial and final states, and $\vec{q}$ is the momentum transfer from the photons to the electrons at positions $\vec{r}$.[26,27] The exponential term can be expanded as $\exp(i\vec{q}\cdot\vec{r})=1+i\vec{q}\cdot\vec{r}+(i\vec{q}\cdot\vec{r})^2/2+\ldots$, where the first term does not contribute due to the orthogonality of the states. At low q values (when $qa\ll 1$, where a is the core electron orbital radius) the second term, i.e., dipole allowed transitions, dominates the spectrum. In the dipole limit the XRS cross section is actually proportional to the x-ray absorption cross section,[21,28,29] making it possible to measure low-energy absorption edges using hard x-rays. With increasing q the higher order terms may contribute considerably, allowing the partition of excitations into final states of different symmetries.

The real-space multiple-scattering code FEFF has been recently extended to calculate XRS spectra.[23,30] Even with the flexibility of the real-space multiple-scattering approach, substitutional systems are still computationally challenging. For example, in the present case the substituting Al atoms randomly occupy some of the Mg lattice sites, and an exact calculation would entail considering all possible symmetry irreducible arrangements in a given cluster. Although basically viable, the large number of involved configurations makes this approach unpractical. Our recent scheme[23,24] to extract the final state ℓDOS (i.e., in the presence of a core hole) from experimental XRS data, however, is directly applicable to doped systems. In this scheme, the only theoretical input is the embedded atom transition matrix elements, which are used to solve the set of linear equations relating the experiment and ℓDOS. Since the transition matrix elements change only little between MgB_2 and AlB_2, the calculation for the pure MgB_2 can be directly applied to the Al-substituted compound.

III. EXPERIMENTAL DETAILS

For the XRS experiment we used two single crystal samples, a $Mg_{0.83}Al_{0.17}B_2$ crystal and a MgB_2 crystal, grown using a high-pressure anvil technique.[10,31] The resulting platelike samples were characterized using magnetization measurements. $Mg_{0.83}Al_{0.17}B_2$ was found to undergo a superconducting transition at 28.2 K, compared to the critical temperature of 39 K in pure MgB_2. The quality and the orientation of the samples were verified using the x-ray Laue technique. MgB_2 crystallizes into the AlB_2 structure with alternating hexagonal Mg and graphitelike B layers running in the ab plane with the c axis perpendicular to these. Al acts as a substitutional impurity, replacing part of the Mg in the lattice and causing a decrease in the Mg-B bond lengths.

The XRS experiment was done at beamline ID16 of the European Synchrotron Radiation Facility. The incident radiation was monochromatized using a Si(111) double-crystal monochromator and focused on the sample by a toroidal mirror into a spot size of roughly 100×100 μm^2. The energies of the scattered photons were analyzed using a spherically bent Si crystal with a bending radius of 1 m, operating in a horizontal Rowland circle scattering geometry.

The XRS spectra from the $Mg_{0.83}Al_{0.17}B_2$ crystal were measured for $q=2.8$ Å^{-1} and 9.8 Å^{-1} with $\vec{q}\|ab$ plane and $\vec{q}\|[001]$ (the c axis). From the pure MgB_2 crystal we measured XRS at low momentum transfer of $q=2.8$ Å^{-1} for $\vec{q}\|ab$ plane and $\vec{q}\|[001]$ using the same setup. We used the inverse energy scan technique,[32,33] where the scattered photons are analyzed at a fixed energy, and the energy transfer is controlled by tuning the incident photon energy. For $q=2.8$ Å^{-1} the scattered photons were analyzed using the Si(444) reflection with a fixed energy of 7907.3 eV, yielding an overall energy resolution of 1.1 eV. At high momentum transfer ($q=9.8$ Å^{-1}) we used the Si(555) reflection from the analyzer crystal with a fixed energy of 9884.8 eV, giving a 1.5 eV overall energy resolution. The spectra were corrected for the smooth inelastic scattering background by approximating it with a single second-degree polynomial.[22] The almost linear background correction does not introduce any spurious features to the spectra, and for the first 40 eV above the threshold, the spectra are largely unaffected by the details of the background removal. High above the threshold, however, the slope of the corrected spectra has some sensitivity to the parameters of the fit.

IV. RESULTS AND DISCUSSION

Figure 1 shows the low momentum transfer XRS spectra. With $\vec{q}\|ab$ plane, the experiment probes mainly the σ symmetry empty electronic states, whereas with $\vec{q}\|[001]$ the empty π states perpendicular to the B planes are reached. The main difference between $Mg_{0.83}Al_{0.17}B_2$ and MgB_2 is the reduction of the intensity in the first peaks above the threshold. The effect can be traced back to the filling of the empty states at the Fermi level due to electron doping induced by the Al substitution. The XRS spectra from the pure MgB_2 are similar to the spectra reported in Ref. 22, which was measured at a smaller momentum transfer of $q=2.1$ Å^{-1}. The slight vertical offset between the two spectra at around 185 eV energy transfer could be possibly partly stemming from background removal and from the lower energy position of the peak around 187 eV in MgB_2 compared to $Mg_{0.83}Al_{0.17}B_2$.

The effect of increasing q is shown in Fig. 2 for the $Mg_{0.83}Al_{0.17}B_2$ crystal. The normalization here is the same as in Ref. 22. In Fig. 2(a), the intensity of the peak at 187.5 eV right above the threshold is decreasing, and the peak at 193.5 eV gains intensity with increasing momentum transfer. In Fig. 2(b), the most striking difference between the low and high momentum transfer spectra is the collapse of the inten-

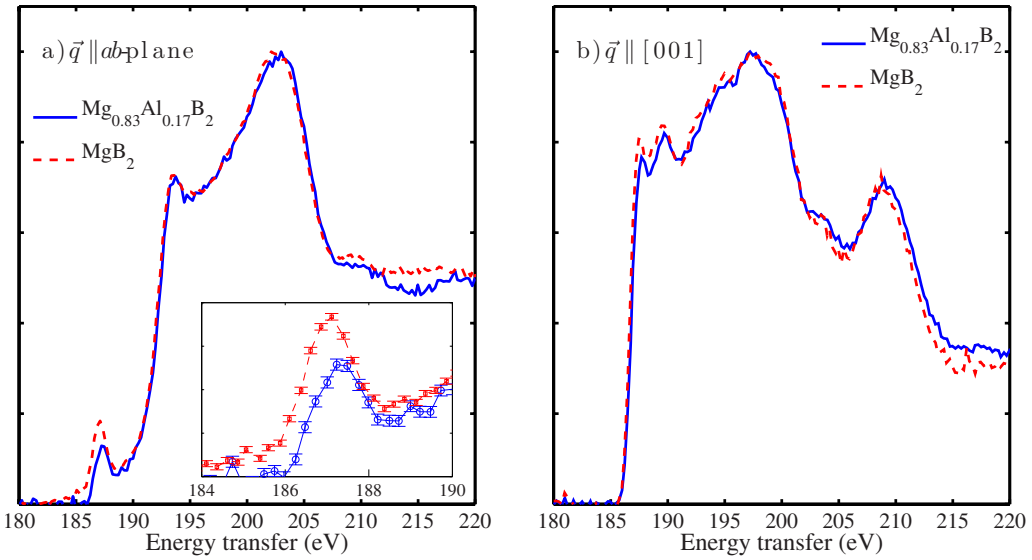

FIG. 1. (Color online) B-K edge x-ray Raman scattering spectra at low momentum transfer (q=2.8 Å^{-1}) from pure MgB_2 (red dashed line) and $Mg_{0.83}Al_{0.17}B_2$ (blue solid line) single crystal samples with (a) momentum transfer $\vec{q}\|ab$ plane and (b) $\vec{q}\|[001]$. The effect of electron doping induced by the Al substitution is seen in the reduced intensity of the first peak in (a) (shown in inset with error bars) and (b).

sity right above the threshold. The B-K threshold q dependence in $Mg_{0.83}Al_{0.17}B_2$ for $\vec{q}\|[001]$ is distinctly different from MgB_2,[22] where the region between 192 and 205 eV gains considerably in intensity with increasing q, while only a small change in the region up to about 5 eV above the edge is observed.

Next, we proceed to extract the ℓDOS for $Mg_{0.83}Al_{0.17}B_2$ using the scheme detailed in Ref. 23. We calculated the atom transition matrix elements and atomic background $S_0(q,\omega)$ (Ref. 23 and 24) with the FEFF code in a MgB_2 cluster with a radius of 8.5 Å (265 atoms), employing the Hedin–Lundqvist exchange correlation potential. We normalized the spectra using the atomic background below threshold to 218 eV for scaling. The normalization process is discussed in detail in Ref. 24. To extract the ℓDOS, the linear equations linking the experiment and the ℓDOS were solved. The results are shown in Fig. 3 for the local density of p symmetry states (pDOS) and in Fig. 4 for the local density of s symmetry states (sDOS), together with MgB_2 ℓDOS from Ref. 24 for comparison. The error bars in the insets in Fig. 3 are calculated from the statistical errors in the x-ray Raman spectra.[34] The position of the Fermi energy was estimated using the value from the calculation and was set to 186.9 eV. The pDOS for $\vec{q}\|ab$ plane shows less holes at the Fermi energy than MgB_2. Otherwise, the pDOS is characterized by a 5-eV gap following the peaked pDOS at the Fermi energy

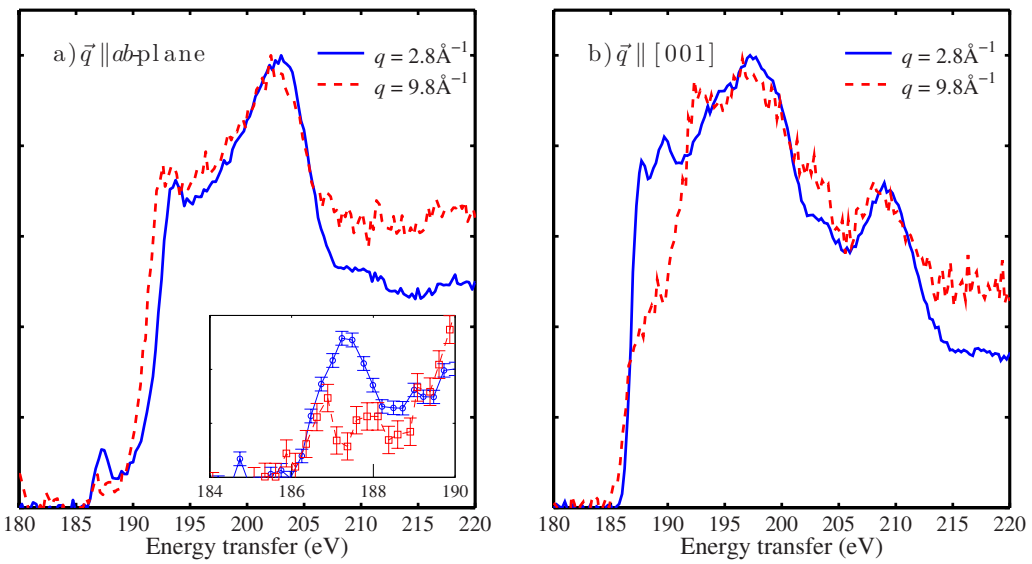

FIG. 2. (Color online) B-K threshold x-ray Raman scattering spectra from $Mg_{0.83}Al_{0.17}B_2$ single crystal at low (blue solid line) and high (dashed red line) momentum transfer with (a) momentum transfer $\vec{q}\|ab$ plane and (b) $\vec{q}\|[001]$. The magnitudes of the momentum transfers are indicated in the figures.

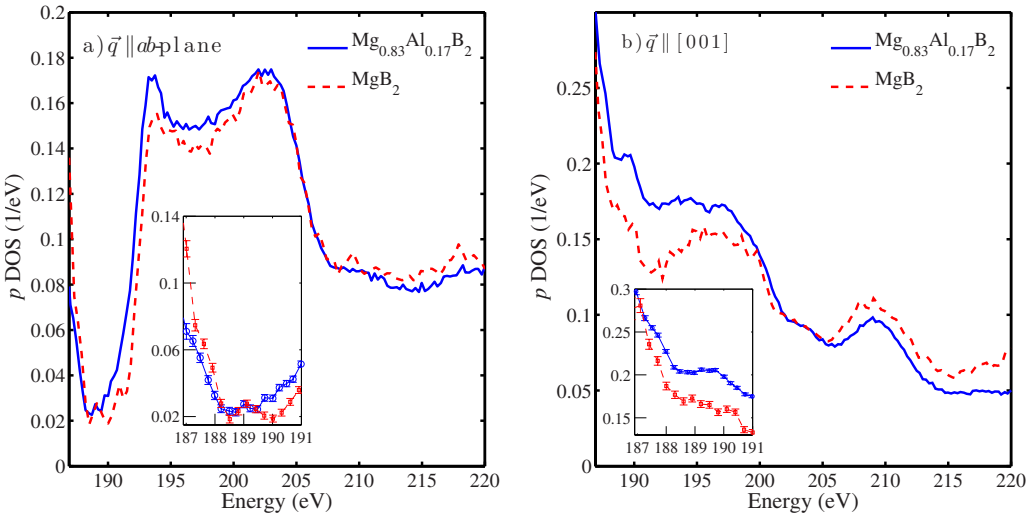

FIG. 3. (Color online) Extracted pDOS for pure MgB_2 (Ref. 24) (red dashed line) and $Mg_{0.83}Al_{0.17}B_2$ (blue solid line). In (a) $\vec{q}\|ab$ plane, in which case mostly σ symmetry final states are reached. In (b) $\vec{q}\|[001]$, leading to excitations into π symmetry final states. The Fermi energy is at 186.9 eV.

as in MgB_2. For $\vec{q}\|[001]$ almost no change in the ℓDOS at the Fermi energy is observed.

To get a more quantitative picture of the differences and to extract the relative hole counts at the Fermi energy, we integrate the pDOS from the Fermi energy (at 186.9 eV) to 188.5 eV for $\vec{q}\|ab$ plane. Some inaccuracies to the absolute hole count can be introduced by broadening effects due to experimental resolution and core hole lifetime.[35] Also, the large value of the first data point on MgB_2 pDOS can complicate the process. The ratio of the hole counts between the $Mg_{0.83}Al_{0.17}B_2$ and MgB_2 pDOS is, however, relatively stable against the exact choice of the Fermi energy and integration range end point, yielding 0.65 ± 0.09. For $\vec{q}\|[001]$, integrating the pDOS from the Fermi energy over a range of 0.5 to 187.4 eV, the hole count ratio gives 1.04 ± 0.07. Despite the aforementioned complications, the final state density for $\vec{q}\|ab$ plane i.e., in the σ band, is clearly more strongly affected by the Al substitution than the hole count in the π band. These conclusions are supported by a recent theoretical work.[36] The stability of the π band hole number at the Fermi energy considering the error estimate, even with 17% Al substitution, would suggest phonon frequency or interband scattering-related effects to be behind the changes in the superconducting energy gap with Al substitution.[9] Even though the extracted ℓDOS is determined in the presence of a core hole, the differences between the final state and ground state pDOS are of the order of 3% at the Fermi energy.

In Fig. 4 the sDOS for $Mg_{0.83}Al_{0.17}B_2$ is slightly different between the two directions, probably partly due to uncertainties in the background correction. However, these possible uncertainties in the slope of the background correction well above the threshold do not affect the determined ℓDOS close to the Fermi energy. As in MgB_2, the Al-substituted sample has almost no sDOS above the Fermi level in an about 4-eV wide region. The main difference between the pure and Al-doped MgB_2 is the collapse of the peak around 192.5 eV. This can be most likely understood beyond the rigid band model, with electron doping shifting band energies besides filling. A FEFF calculation of the final state sDOS for AlB_2 and MgB_2 supports this conclusion, showing AlB_2 to have less empty states at the 192.5 eV peak.

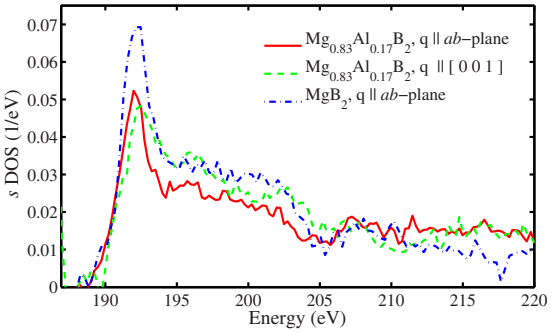

FIG. 4. (Color online) Extracted sDOS for MgB_2 (blue dot-dash line) (Ref. 24) for $\vec{q}\|ab$-plane spectra, and for $Mg_{0.83}Al_{0.17}B_2$ for $\vec{q}\|[001]$ (green dashed line) and for $\vec{q}\|ab$ plane (red solid line). The Fermi energy is at 186.9 eV.

V. CONCLUSIONS

In summary, we have measured XRS spectra at the B-K edge from $Mg_{0.83}Al_{0.17}B_2$ and MgB_2 single crystals. We have extracted the different components of the local density of states in the final state of the scattering process for $Mg_{0.83}Al_{0.17}B_2$. We observe the filling of the B-σ band due to electron doping of the system induced by the Al substitution, with a hole count ratio of 0.65 ± 0.09 relative to MgB_2 at the Fermi energy. The B-π band hole number at the Fermi energy stays constant within the error estimate. Our results further demonstrate the power of utilizing the q dependence of XRS combined with state of the art first-principles calculations, allowing the extraction of site and symmetry projected density of states in substituted and doped systems.

ACKNOWLEDGMENTS

We thank M. Hakala for invaluable discussions. This work was supported by the Academy of Finland (Contract No. 201291/205967/110571) and by the Swiss National Science Foundation through the NCCR pool MaNEP.

*Aleksi.Mattila@stuk.fi

[1] J. Nagamatsu, N. Nakagawa, T. Muranaka, Y. Zenitani, and J. Akimitsu, Nature (London) **410**, 63 (2001).
[2] A. Y. Liu, I. I. Mazin, and J. Kortus, Phys. Rev. Lett. **87**, 087005 (2001).
[3] H. J. Choi, D. Roundy, H. Sun, M. L. Cohen, and S. G. Louie, Nature (London) **418**, 758 (2002); H. J. Choi, D. Roundy, H. Sun, M. L. Cohen, and S. G. Louie, Phys. Rev. B **66**, 020513(R) (2002).
[4] I. I. Mazin, O. K. Andersen, O. Jepsen, O. V. Dolgov, J. Kortus, A. A. Golubov, A. B. Kuzmenko, and D. van der Marel, Phys. Rev. Lett. **89**, 107002 (2002).
[5] For a review, see special issue on MgB_2, Physica C **385**, 1 (2003).
[6] J. M. An and W. E. Pickett, Phys. Rev. Lett. **86**, 4366 (2001).
[7] T. Yildirim, O. Gulseren, J. W. Lynn, C. M. Brown, T. J. Udovic, Q. Huang, N. Rogado, K. A. Regan, M. A. Hayward, J. S. Slusky, T. He, M. K. Haas, P. Khalifah, K. Inumaru, and R. J. Cava, Phys. Rev. Lett. **87**, 037001 (2001).
[8] R. S. Gonnelli, D. Daghero, G. A. Ummarino, A. Calzolari, M. Tortello, V. A. Stepanov, N. D. Zhigadlo, S. M. Kazakov, and J. Karpinski, J. Supercond. **18**, 681 (2005).
[9] R. S. Gonnelli, D. Daghero, G. A. Ummarino, A. Calzolari, V. Dellarocca, V. A. Stepanov, S. M. Kazakov, J. Jun, and J. Karpinski, J. Phys. Chem. Solids **67**, 360 (2006).
[10] J. Karpinski, N. D. Zhigadlo, G. Schuck, S. M. Kazakov, B. Batlogg, K. Rogacki, R. Puzniak, J. Jun, E. Muller, P. Wagli, R. Gonnelli, D. Daghero, G. A. Ummarino, and V. A. Stepanov, Phys. Rev. B **71**, 174506 (2005).
[11] S. M. Kazakov, R. Puzniak, K. Rogacki, A. V. Mironov, N. D. Zhigadlo, J. Jun, C. Soltmann, B. Batlogg, and J. Karpinski, Phys. Rev. B **71**, 024533 (2005).
[12] J. S. Slusky, N. Rogado, K. A. Regan, M. A. Hayward, P. Khalifah, T. He, K. Inumaru, S. M. Loureiro, M. K. Haas, H. W. Zandbergen, and R. J. Cava, Nature (London) **410**, 343 (2001).
[13] J. Kortus, O. V. Dolgov, R. K. Kremer, and A. A. Golubov, Phys. Rev. Lett. **94**, 027002 (2005).
[14] A. Carrington, J. D. Fletcher, J. R. Cooper, O. J. Taylor, L. Balicas, N. D. Zhigadlo, S. M. Kazakov, J. Karpinski, J. P. H. Charmant, and J. Kortus, Phys. Rev. B **72**, 060507(R) (2005).
[15] R. J. Cava, H. W. Zandbergen, and K. Inumaru, Physica C **385**, 8 (2003).
[16] H. D. Yang, H. L. Liu, J.-Y. Lin, M. X. Kuo, P. L. Ho, J. M. Chen, C. U. Jung, M.-S. Park, and S.-I. Lee, Phys. Rev. B **68**, 092505 (2003).
[17] L. D. Cooley, A. J. Zambano, A. R. Moodenbaugh, R. F. Klie, J.-C. Zheng, and Y. Zhu, Phys. Rev. Lett. **95**, 267002 (2005).
[18] R. F. Klie, J. C. Zheng, Y. Zhu, A. J. Zambano, and L. D. Cooley, Phys. Rev. B **73**, 014513 (2006).
[19] J. Nakamura, S. Y. Nasubida, E. Kabasawa, H. Yamazaki, N. Yamada, K. Kuroki, M. Watanabe, T. Oguchi, S. Lee, A. Yamamoto, S. Tajima, Y. Umeda, S. Minakawa, N. Kimura, H. Aoki, S. Otani, S. Shin, T. A. Callcott, D. L. Ederer, J. D. Denlinger, and R. C. C. Perera, Phys. Rev. B **68**, 064515 (2003).
[20] D. Di Castro, M. Ortolani, E. Cappelluti, U. Schade, N. D. Zhigadlo, and J. Karpinski, Phys. Rev. B **73**, 174509 (2006).
[21] Y. Mizuno and Y. Ohmura, J. Phys. Soc. Jpn. **22**, 445 (1967).
[22] A. Mattila, J. A. Soininen, S. Galambosi, S. Huotari, G. Vanko, N. D. Zhigadlo, J. Karpinski, and K. Hämäläinen, Phys. Rev. Lett. **94**, 247003 (2005).
[23] J. A. Soininen, A. L. Ankudinov, and J. J. Rehr, Phys. Rev. B **72**, 045136 (2005).
[24] J. A. Soininen, A. Mattila, J. J. Rehr, S. Galambosi, and K. Hämäläinen, J. Phys.: Condens. Matter **18**, 7327 (2006).
[25] T. A. Callcott, L. Lin, G. T. Woods, G. P. Zhang, J. R. Thompson, M. Paranthaman, and D. L. Ederer, Phys. Rev. B **64**, 132504 (2001).
[26] W. Schülke, in *Handbook of Synchrotron Radiation*, edited by G. S. Brown and D. E. Moncton (North-Holland, Amsterdam, 1991), Vol. 3.
[27] K. Hämäläinen and S. Manninen, J. Phys.: Condens. Matter **13**, 7539 (2001).
[28] H. Nagasawa, S. Mourikis, and W. Schülke, J. Phys. Soc. Jpn. **66**, 3139 (1997).
[29] S. Manninen and K. Hämäläinen, Phys. Rev. B **45**, 3878(R) (1992).
[30] A. L. Ankudinov, B. Ravel, J. J. Rehr, and S. D. Conradson, Phys. Rev. B **58**, 7565 (1998).
[31] J. Karpinski, M. Angst, J. Jun, S. M. Kazakov, R. Puzniak, A. Wisniewski, J. Roos, H. Keller, A. Perucchi, L. Degiorgi, M. R. Eskildsen, P. Bordet, L. Vinnikov, and A. Mironov, Supercond. Sci. Technol. **16**, 221 (2003).
[32] W. Schülke and H. Nagasawa, Nucl. Instrum. Methods Phys. Res. A **222**, 203 (1984).
[33] K. Hämäläinen, S. Manninen, C.-C. Kao, W. Caliebe, J. B. Hastings, A. Bansil, S. Kaprzyk, and P. M. Platzman, Phys. Rev. B **54**, 5453 (1996).
[34] S. Galambosi, J. A. Soininen, K. Nygård, S. Huotari, and K. Hämäläinen, Phys. Rev. B **76**, 195112 (2007).
[35] A. L. Ankudinov, A. I. Nesvizhskii, and J. J. Rehr, J. Synchrotron Radiat. **8**, 92 (2001).
[36] F. Bernardini and S. Massidda, Phys. Rev. B **74**, 014513 (2006).